

Determination of Tucson, Arizona as an Ecological Trap for Cooper's Hawks (*Accipiter cooperii*)

Jouie Ames¹, Andrea Feiler², Giancarlo Mendoza³, Adam Rumpf², Stephen Wirkus²

¹University of California, Santa Cruz, ²Arizona State University, ³Universidad Metropolitana P.R.

August 2011

Abstract

The term “ecological trap” has been used to describe a habitat in which its attractiveness has been disassociated with its level of suitability. To date, fewer than ten clearly delineated examples of them have been found; they are either rare in nature, hard to detect, or a combination of both. It has been hypothesized that the city of Tucson, Arizona is an ecological trap for Cooper's Hawks (*Accipiter cooperii*) due to the abundance of prey species, namely columbids, which make up over 80% of the hawk's diet. Overall, more than 40% of these columbid populations are carriers of the protozoan *Trichomonas gallinae*, which directly contributes to a nestling mortality rate of more than 50% in the hawks. Using an epidemiological framework, we create two SIR-type models, one stochastic and one deterministic, utilizing parameter estimates from more than ten years of data from the dove (columbid) and hawk populations in the city. Through mathematical modeling and bifurcation theory, we found that the proportion of infected columbids, does not have an effect on classifying Tucson as an ecological trap for Cooper's Hawks, but by increasing the disease death rate, it can be considered an ecological trap.

1 Introduction

When the term “ecological trap” was first coined in 1972 by Dwernychuk and Boag [1], it was originally used to describe a natural trap in ones habitat but now is used almost exclusively to refer to anthropogenically induced traps [1,2]. Ecological traps are a subset of evolutionary traps and it is important to note that both are behavioral rather than population phenomena [3]. The following definitions are currently in use:

- **Sink:** a habitat that supports negative population growth even at small population densities, (i.e., the population is in decline) [4].
- **Source-sink:** animals occupy high-suitability areas first then less suitable areas; results in zero net population growth overall (i.e., the population size remains unchanged) [5].
- **Ecological trap:** a sink habitat that is preferred above more suitable available habitats [3].
- **Evolutionary trap:** a habitat that provides misleading perceptual cues such that the organism makes maladaptive behavioral or life-history choices [3].

In 2006, Robertson and Hutto performed a survey of literature related to ecological traps and found 45 hypothesized cases (37 avian, 5 insect, 2 mammal and 1 reptile) and of these, only four provided sufficient empirical data to classify the population as being caught in an ecological trap [6]. By 2010, Robertson et al. found fewer than 10 clear-cut examples [7]. One incontrovertible example is that of the caddis fly (*Hydropsyche pellucidula*) [8]. Caddis flies are polarotactic insects and the adults are lured away from water sources to glass buildings by the polarization of light; they mate on the windows and lay their eggs in the crevices surrounding the panes. This is a wholly unsuitable environment for the eggs to develop and they experience complete mortality [7,8]. Also, the adults are unable to escape due to the polarization captivity effect [7]. This situation has the potential to become an ecological trap for other species as well. As Kriska noted in 2010 [8], numerous bird species are now feeding on these trapped insects, and it has been found that glass buildings cause the death of at least hundreds of thousands of birds over the course of a year [9,10]. Thus these buildings have the potential to be a multi-species ecological trap.

As illustrated above with the caddis fly, one of the driving forces for the evolution of species is habitat selection, whether it is for feeding, breeding, or other life-history events. Animals that select environments for which they are best suited have a higher fitness than those choosing less suitable areas [6]. Animals frequently rely on environmental cues for habitat selection (i.e. polarized light sources, prey availability, etc.); these cues may not be directly related to the suitability of the area for the species making the choice [3]. Thus, where an ecological trap exists there is no correlation between the cues animals rely on as indicators of suitability and the actual suitability of the environment. Robertson and

Hutto [6] classify ecological traps into two distinct categories: equal-preference and severe ecological traps. These ecological traps are determined based on which of the following three mechanisms are involved:

1. There is an increase in the attractiveness of an area without a change in the suitability (equal-preference).
2. The attractiveness remains stable but there is a decrease in suitability (equal-preference).
3. There is an increase in the attractiveness of the area with a decrease in the suitability (severe).

Robertson and Hutto then contend that in order for an area to be sufficiently classified as an ecological trap for a species, it must meet the following three criteria:

1. Individuals must exhibit a preference (in the case of severe) or at least equal preference for the area.
2. There must be a surrogate measure of fitness that shows a difference in fitness between individuals from the area under study and individuals from other populations.
3. The fitness outcome in the preferred area must be lower in the preferred habitat than in other habitats.

Most of the ecological traps cited by Robertson are the direct result of habitat fragmentation and the resulting proliferation of ecotones (the areas of transition between two distinct habitats such as where a field meets a forest). These heterogeneous areas typically support high biodiversity [11–13] but may in fact be ecological traps for species due to increased predation rates in these areas [14, 18]. To illustrate this point, Weldon and Haddad found that Indigo buntings were attracted to areas with increased anthropogenic edge area, but nesting in these edge areas resulted in significantly fewer fledges per nest than in more compact areas with less edge area [15], thus the areas are ecological traps for the buntings.

Since the publication of Robertson and Hutto’s 2006 article outlining the criteria for determining an ecological trap, numerous authors have applied this criteria to test for it with varying results. Zugmeyer and Koprowski found, through statistical analysis, that the insect damaged forests of Mt. Graham in southern Arizona did meet the criteria for an ecological trap for red squirrels (*Tamiasciurus hudsonicus grahamensis*) [16]. These squirrels exhibit equal-preference for insect damaged forests, but have lower survivorship and reproductive success than in unaffected forests. There does appear to be a threshold of damaged they can tolerate; all the forests they inhabit have less 69% dead trees [16]. However, most researchers report their populations meet some of the criteria but not others. For example, Igual et al. studied whether the “presence of an alien nest predator” is used as an environmental cue in breeding site selection by Cory’s shearwater (*Calonectris*

diomeda). They found that there was no uncoupling of environmental cues from the suitability of the environment even though there was a difference in preference [17].

Loss of habitat is also frequently cited as a major factor in the decline or extinction of numerous species [19–22], yet some species are flourishing rather than declining as they become adapted to life in cities [27–29]. In 2005, Arizona was determined to have the fourth largest human population growth rate in the United States and hundreds of thousands of acres of grazing lands are being converted annually to urban and suburban areas due to urban sprawl [23]. Whereas this may spell disaster for many species, two species of columbids, Mourning doves (*Zenaida Macroura*) and Inca doves (*Columbina Inca*), are adapting well and their population numbers are swelling with increased urbanization [24,25]. However, in the city of Tucson, overall, more than 40% of the dove populations are carriers of the protozoan *Trichomonas gallinae*, which causes the disease trichomoniasis, also known as frounce in raptors and canker in columbids, though columbids are primarily asymptomatic carriers of the parasite [26].

Cooper’s hawks are avivorous predators and in Tucson, up to 83% of their diet is comprised of columbids [34,35]; *T. Gallinae* is transferred to the hawk nestlings when the parents feed them meat from an infected columbid [34]. The hawks have an overall nestling mortality rate of more than 50%, of which 87% is directly attributable to the disease [34]. Thus, the hawks may be lured into the area by the abundance of prey species [24], but this could be considered an ecological trap if the prey is sufficiently infected such that they cause a net population growth less than one. While *T. gallinae* does not have distinct intermediate and definitive hosts, many parasites infect intermediate hosts and cause them to select ecological traps in order to complete their life cycle. For example, *Toxoplasma gondii* causes infects rats brains and causes them to seek out cats [32], *Dicrocoelium dendriticum* infects ants brains and cuses them to cling to the tops of grass to be eaten by herbivores [31], and *Euhaplorchis californiensis* causes killifish (*Fundulus parvipinnis*) to swim at the surface of the water making them easy prey for birds [30]. These are just three examples of a parasite altering the brain function of a species and making them enter a life threatening situation; the ultimate ecological trap.

Our research focuses on the population of Cooper’s hawks living in Tucson, that feed primarily on these doves. This hawk population has been studied extensively by Boal, Mannan and other researchers at the University of Arizona for more than 10 years (1994–2008) [33–40]. In 1997, Boal completed his PhD. dissertation and came to the conclusion that Tucson was an ecological trap for Cooper’s hawks [33]; he contended that the Tucson Cooper’s hawk population was being maintained by the immigration of hawks from other regions into Tucson, Arizona. Yet, in his later study (2008) he found that while the nestling mortality is high, first over-wintering mortality rates in the city were sufficiently low to allow a fecundity greater than one, and thus the population is self-sustaining [35]. He came to this conclusion after 10 more years of studying the population and using banding/resighting techniques as well as radio-tagging some of the individuals. For the later study he created ten population models using the software MARK and used Akaike’s Information Criterion “to distinguish the exploratory power of the models”. He then

employed Leslie matrices to determine the rate of population change and concluded Tucson is not a sink for the hawk population [35].

The goal of our study is to create mathematical models that will allow us to investigate the infection rate in columbids that would allow Tucson to fit the definition of an ecological trap and meet Robertson and Hutto's criteria. The population currently meets the first criteria of the hawks preferring the city as opposed to the exurban areas surrounding it. In the desert areas surrounding the city, Cooper's hawks feed on a wider variety of prey species and the columbid infection rates are much lower [35], thus reducing the probability of the nestlings becoming infected. Still, due to the abundance of prey and availability of nesting sites, the city appears more attractive than the surrounding areas. After determining the infection rate that would reduce the growth rate to less than one, the second and third criteria would be met. We will approach the population dynamics of Cooper's hawks using a deterministic model in section 2.1, its analysis in 2.2 and then results in section 2.3, a stochastic model in section 3.1, an extension of the stochastic model in 3.2. We will then analyze these models in section 3.3 and 3.4, respectively, by evaluating the parameters in our models to determine the thresholds at which they would cause the Cooper's hawk population to decline.

2 Deterministic Model

2.1 Formulation

For the purposes of our research, we will analyze the Cooper's hawk population in Tucson using a modified SIR-type model with the parasite, *T. Gallinae*, implicitly incorporated via disease infection rate in the columbids population. Columbids comprise more than 80% of the Cooper's hawk's diet in Tucson [42]. We do not explicitly model the columbid populations due to their numbers being in the tens of millions in Arizona [24]; thus, prey availability is assumed not to be a limiting factor in Cooper's Hawk population size and the sole effect the columbids have on the raptor population is the transmission of *T. gallinae*. For our deterministic SIR-type model, we model the Cooper's hawk population in four different compartments: susceptible juveniles (S), infected juveniles (I), recovered juveniles (R), and adult hawks (H). Less than 2% of the adult hawk population is infected by the disease [34]; thus, we assume the effect of the disease on the adult population is sufficiently small such that we do not model it explicitly.

The rate for which juvenile hawks enter the system (hatchling rate), being susceptible, is given by βH because the number of juveniles depends on the total number of adult hawks nesting in the area. The rate of leaving the susceptible class by infection is stated by $\rho\sigma$, where ρ would be the infection rate from infected food and σ is the average proportion of infected doves, calculated from the infection prevalence for each dove species weighted by the species' contribution to the hawks' diet. We incorporate aging factors, α_S and α_R , which will be applied to the susceptible and recovered classes respectively. When the juvenile hawks are infected, they either die of the disease or move into the recovered class.

There is no evidence of the disease halting the maturity of the juvenile hawks and the infection period is relatively short to the juvenile hawk's maturity period; hence we will assume $\alpha_R = \alpha_S$. Dying from the disease is denoted by the rate d and recovering from it is γ . The natural death rates for the juvenile and adult hawks are denoted by μ_j and μ_H , respectively. The immigration rate in the adult class is given by $\frac{\Lambda}{H}$. See Table 1 for the list of parameters, and their definitions and values. Figure 1 depicts the life cycle of juvenile hawks from hatch time to death.

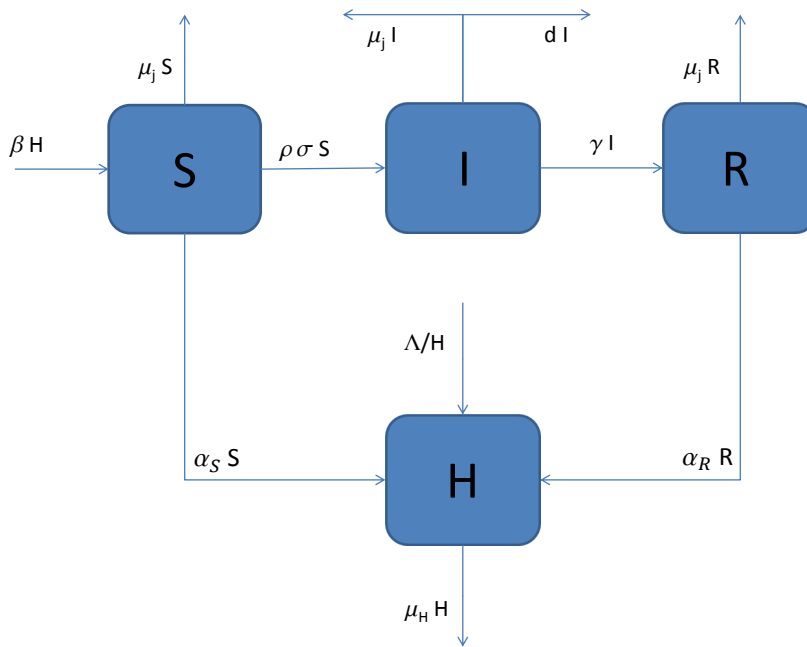


Figure 1: SIR-type model with an aged class, H . The arrows represent transfers between classes, with flow rates given by the corresponding expressions.

With the assumption of α_R being equal to α_S , we will simply denote α_S as α . From Figure 1, we get the following system of ordinary differential equations:

$$\dot{H} = \alpha(S + R) - \mu_H H + \frac{\Lambda}{H} \quad (1)$$

$$\dot{S} = \beta H - (\rho\sigma + \mu_j + \alpha)S \quad (2)$$

$$\dot{I} = \rho\sigma S - (\mu_j + d + \gamma)I \quad (3)$$

$$\dot{R} = \gamma I - (\mu_j + \alpha)R \quad (4)$$

Cooper's hawks are territorial birds: the number of immigrants is limited by the number of hawks already living in an area, and therefore the immigration rate into Tucson is given by $\frac{\Lambda}{H}$ [37,51]. The rate at which the susceptibles get infected is denoted for $\rho\sigma$, where ρ is (number of prey per day) \times (proportion of food that is a columbid) \times (probability of getting the infection given that the food is infected) \times (proportion of a prey that is infected), each value was found in literature [35,42,48]. It should be noted that the probability of transmission determined by Stabler [48] is the maximum probability of getting the infection after being exposed to the pathogen; *T. gallinae* was swabbed directly onto the oral mucosa of the hawks. The value of σ was calculated from the proportion of the prey species (Inca, Mourning, and White-winged doves) that are infected [26,41], as well as the proportion of each prey species that makes up the hawks' diet [42].

The aging factor, α , is estimated to be two years (the average time it takes a hawk to reach sexual maturity), therefore it's given by $\frac{1}{365 \cdot 2}$. As found in [35], the juvenile hawks become largely immune to the disease after 40 days. This gives us a disease death rate d of $\frac{0.41}{40}$, which means that 41% of the population dies during the period of the infection. From this we know that 59% recover from the disease, thus γ is $\frac{0.59}{40}$. Juvenile hawks have a 64% percent survival rate, giving a natural death rate of $\mu_j = \frac{0.36}{365 \cdot 2}$. Since the Cooper's hawks live, on average, seven years and they live two years before becoming adults; the adults' natural death rate can be denoted as $\mu_H = \frac{1}{365 \cdot 5}$. Finally β , the hawk birth rate, is the number of hatchlings per nest per breeding hawk per year, which numerically is $\frac{3.44}{365 \cdot 2} \cdot 0.66 \cdot 0.835$. The $\frac{3.44}{365 \cdot 2}$ represents that on average they produce 3.44 offspring per nest [35] and there are two adult hawks per nest per year. The proportion of adults that breed in any given year is 0.66, and the 0.835 term compensates for the 16.5% rate of pre-hatching nest failures [33].

2.2 Model Analysis

In analyzing our system (1)-(4), we wish to find biologically relevant equilibrium points (in which all the values of the equilibrium are non-negative). To do so, we set each of the population equations equal to 0 and solve for H , S , I , and R . We first note that there is no disease free equilibrium (DFE), i.e. a solution in which $I = 0$, due to the immigration term $\frac{\Lambda}{H}$ in (1). Hence, there is only an endemic equilibrium (EE) for our system (1)-(4),

Table 1: Parameters' definition, values and source

Parameter	Definition	Value	Source
Λ	Hawk immigration rate	1	approx.
ρ	Transmission constant	0.246	(see parameter explanation)
α	Hawk aging rate	$\frac{1}{365 \cdot 2}$	[35]
d	Hawk disease death rate	$\frac{0.41}{40}$	[33]
μ_H	Adult hawk natural mortality rate	$\frac{1}{365 \cdot 5}$	approx.
μ_j	Juvenile hawk natural mortality rate	$\frac{0.36}{365 \cdot 2}$	[35]
γ	Recovery rate of juvenile hawks	$\frac{0.59}{40}$	approx.
σ	Weighted average proportion of infected doves	0.423	[26]
β	Hawk hatch rate	0.00268	[35]

which is given by (see Appendix A):

$$H^* = \left(\frac{\Lambda}{\mu_H - \alpha \left[1 + \frac{\gamma \rho \sigma}{(\mu_j + \alpha)(\mu_j + d + \gamma)} \right] \left[\frac{\beta}{\mu_j + \rho \sigma + \gamma} \right]} \right)^{\frac{1}{2}}, \quad (5)$$

$$S^* = \frac{\beta H^*}{\mu_j + \rho \sigma + \alpha}, \quad (6)$$

$$I^* = \frac{\beta \rho \sigma H^*}{(\mu_j + d_j + \gamma)(\mu_j + \rho \sigma + \alpha)}, \quad (7)$$

$$R^* = \frac{\gamma \beta \rho \sigma H^*}{(\mu_j + \alpha)(\mu_j + d_j + \gamma)(\mu_j + \rho \sigma + \alpha)}. \quad (8)$$

Because we need $H^* > 0$, the denominator in (5) gives the condition:

$$\alpha \left(1 + \frac{\gamma \rho \sigma}{(\mu_j + \alpha)(\mu_j + d + \gamma)} \right) \left(\frac{\beta}{\mu_j + \rho \sigma + \gamma} \right) < \mu_H. \quad (9)$$

If this inequality holds, then the equilibrium exists and is biologically relevant, as all the parameters are positive. We will assume this inequality holds true from now on. This condition can also be written as:

$$H^* \text{ is biologically relevant } \iff \left(\frac{\alpha}{\mu_H} \right) \left(\frac{\beta}{\mu_j + \rho \sigma + \alpha} \right) + \left(\frac{\alpha}{\mu_H} \right) \left(\frac{\beta}{\mu_j + \rho \sigma + \alpha} \right) \left(\frac{\rho \sigma}{\mu_j + d + \gamma} \right) \left(\frac{\gamma}{\mu_j + \alpha} \right) < 1 \quad (10)$$

This step was done to better understand the behavior of our condition. The factors presented in (10) are interpreted as: $\frac{\alpha}{\mu_H}$, where α is the rate where the juvenile hawks age into the adult class and $\frac{1}{\mu_H}$ is their average time being adults. The next term is $\frac{\beta}{\mu_j + \rho\sigma + \alpha}$, β is the average hatchling rate and it's multiplied by $\frac{1}{\mu_j + \rho\sigma + \alpha}$ which in our model is the average time spent being susceptible. $\frac{\rho\sigma}{\mu_j + d + \gamma}$ can also be separated and we get $\rho\sigma$ which is the transmission rate of the disease, and $\frac{1}{\mu_j + d + \gamma}$ is the average infected period. Lastly we have $\frac{\gamma}{\mu_j + \alpha}$, which is the recovery rate, γ , multiplied by the average period spent in the recovered class, $\frac{1}{\mu_j + \alpha}$. Thus, the whole term is defined as being the average adult population growth rate with contributing terms based on the susceptible and recovered classes.

In order to classify the local stability of this endemic equilibrium, we must first linearize our system (1)-(4), i.e., find the Jacobian, and substitute the equilibrium given by (5)-(8). The Jacobian takes the form:

$$J_{(H^*, S^*, I^*, R^*)} = \begin{bmatrix} -\mu_H - \frac{\Lambda}{(H^*)^2} & \alpha & 0 & \alpha \\ \beta & -(\rho\sigma + \mu_j + \alpha) & 0 & 0 \\ 0 & \rho\sigma & -(\mu_j + d + \alpha) & 0 \\ 0 & 0 & \gamma & -(\mu_j + \alpha) \end{bmatrix} \quad (11)$$

After making the following simplifications:

$$c_1 = \rho\sigma + \mu_j + \alpha, \quad c_2 = \mu_j + d + \alpha, \quad c_3 = \mu_j + \alpha, \quad (12)$$

$$A = -2\mu_H + \frac{\beta\alpha(c_2c_3 + \gamma\rho\sigma)}{c_1c_2c_3}. \quad (13)$$

Equation (11) then reduces to

$$J_{(H^*, S^*, I^*, R^*)} = \begin{bmatrix} A & \alpha & 0 & \alpha \\ \beta & -c_1 & 0 & 0 \\ 0 & \rho\sigma & -c_2 & 0 \\ 0 & 0 & \gamma & -c_3 \end{bmatrix}. \quad (14)$$

The eigenvalues of (14) are very complicated and we were not able to gain any insight into the stability of the EE by examining them. Instead, we will use the Routh-Hurwitz criterion for $n = 4$ in order to test the local stability of our equilibrium. The conditions to be tested, given a fourth order characteristic polynomial, $\lambda^4 + a_1\lambda^3 + a_2\lambda^2 + a_3\lambda + a_4$, are as follows:

Assume $a_1, a_2, a_3, a_4 \in \mathbb{R}$.

Given our EE, it is locally asymptotically stable if and only if

- $a_1 > 0, a_3 > 0, a_4 > 0$
- $a_1a_2a_3 > a_3^2 + a_1^2a_4$

For our endemic equilibrium, we obtain the characteristic polynomial:

$$\lambda^4 + (c_1 + c_2 + c_3 - A)\lambda^3 + (c_1c_2 + c_2c_3 + c_1c_3 - (c_1 + c_2 + c_3)A - \beta\alpha)\lambda^2 + (c_1c_2c_3 - (c_1c_2 + c_2c_3 + c_1c_3)A - \beta\alpha(c_2 + c_3))\lambda - (c_1c_2c_3A + \beta\alpha c_2c_3 + \beta\rho\sigma\alpha\gamma) .$$

Since we assume (9) holds, a_1, a_3 , and a_4 are positive (see Appendix B for a detailed explanation). Thus, we only need to be concerned with the condition $a_1a_2a_3 > a_3^2 + a_1^2a_4$. The following conditions must hold in order to make the inequality true (see Appendix B):

$$\begin{aligned} a_3 &< a_1a_2 & (15) \\ a_4a_1^2 &< ((c_1 + c_2 + c_3)(c_1c_2 + c_2c_3 + c_1c_3 - Aa_1) + \beta\alpha(A - c_1) - c_1c_2c_3)a_3, & (16) \end{aligned}$$

with c_1, c_2, c_3 and A given by (12)-(13). If our EE meets the above conditions, then, by the Routh-Hurwitz criterion, it is locally asymptotically stable; otherwise, the equilibrium is unstable.

As an alternative way to determine the stability of our EE, we can calculate the characteristic equation and look for $\lambda = 0$ bifurcation or $\lambda = i\omega$ bifurcation (i.e., a Hopf bifurcation). When we substitute $\lambda = 0$ into the general characteristic equation, we obtain the condition

$$H^* = \pm\sqrt{-(H^*)^2} \quad (17)$$

(see Appendix C). Since H^* can never be zero in our model (because $\Lambda > 0$), this condition can clearly never hold. Thus, we cannot have any $\lambda = 0$ bifurcations of the EE in our system.

To determine whether we can have any Hopf bifurcations, we substitute $\lambda = i\omega$ into the characteristic equation. Equating real and imaginary parts, we obtain a complicated implicit equation involving all the parameters. When we vary d and γ and fix all the remaining parameters, we can plot the implicit Hopf bifurcation curves in the d - γ parameter space. However, there are no such curves in the first quadrant, i.e., when both d and γ are positive. Thus we cannot have any Hopf bifurcations in our system since we require $d, \gamma > 0$. Thus our EE does not change stability for any $H^* > 0$.

2.3 Results

Based on our current model and parameter estimates from the literature there does not exist $\sigma \in [0, 1]$ such that there would be a biologically relevant equilibrium in our system. For our model, if there is no equilibrium in \mathbb{R} , population decrease is impossible. As a result, our overall hawk population increases exponentially, regardless of the proportion of columbids infected with *T. Gallinae*. Regardless of the initial number of hawks in each class, the population exponentially increases as long as each class of hawks exists. Thus, with our current parameters, it is unlikely for the hawks to become extinct. However, if we vary our disease death rate, d , then, if d is at least $\frac{0.73}{40}$ (this would reduce the rate of

recovered hawks to $\frac{0.27}{40}$ or less), then, except for very low σ values, our endemic equilibrium exists and satisfies the Routh-Hurwitz criterion; hence, the endemic equilibrium is locally asymptotically stable. This effect is illustrated in Figure 10.

When d is varied from $\frac{0.73}{40}$ (see Figure 3) to $\frac{0.74}{40}$ (see Figure 4), we see that as d increases it takes less time for the population to reach their stable value.

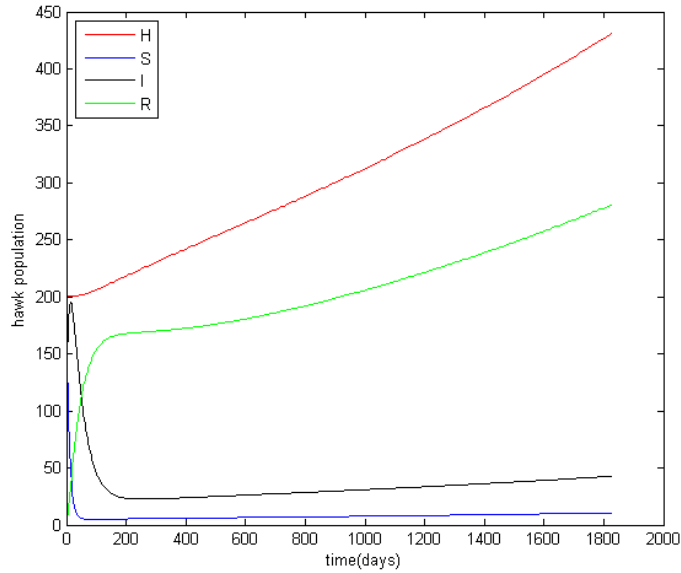


Figure 2: Solution curve of system with initial conditions: $H = 200$, $S = 200$, $I = 100$, $R = 0$. Parameter values may be found in Table 1. EE does not exist.

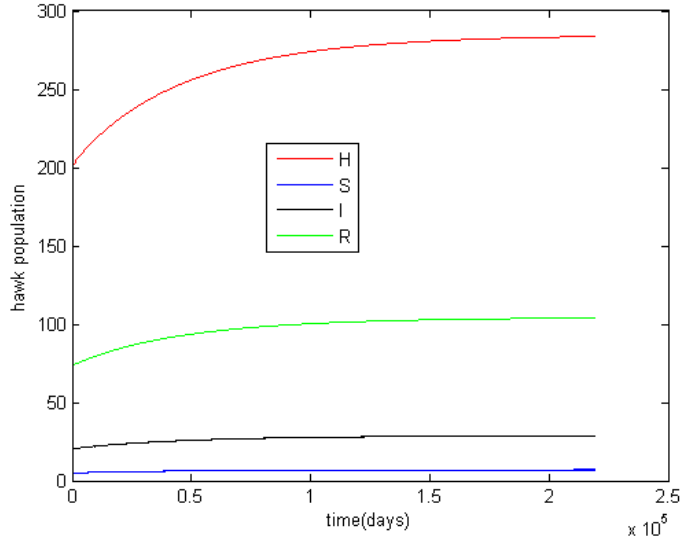


Figure 3: Solution curve of system with initial conditions: $H = 200$, $S = 200$, $I = 100$, $R = 0$; d is changed to $\frac{0.73}{40}$. Note that this graph is plotted over the course of 600 years. EE exists as the adult hawk population approaches 300.

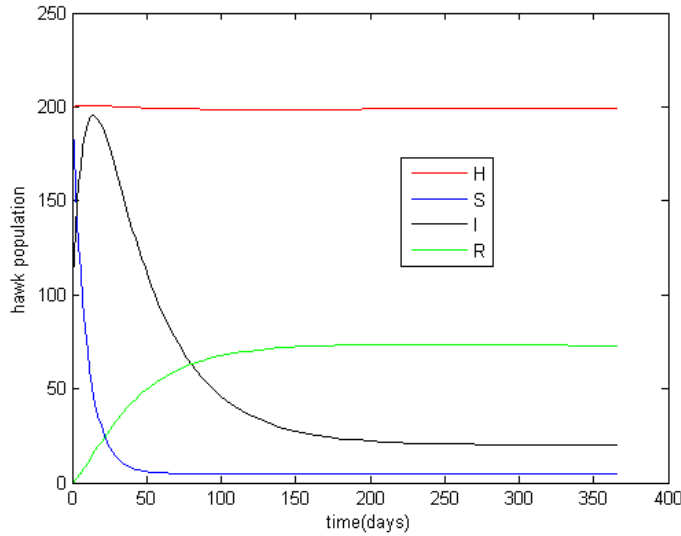


Figure 4: Solution curve of system with initial conditions: $H = 200$, $S = 200$, $I = 100$, $R = 0$; d is changed to 0.7440. There exists an EE for our corresponding d value. Compared to Figure 3, it takes only a year for the population to reach the stability.

In taking an alternative approach, we will vary the average hatchling rate (β), the disease mortality rate of the juvenile hawks (d), and the proportion of columbids infected (σ). The combination of varying these parameters will allow us to understand when our endemic equilibrium exists.

We will first vary β in terms of σ . From observing (6), (7), and (8), we only need to analyze the existence of (5) because each of them is dependent on H^* . Thus, we only need to find the range of values for σ and β such that H^* exists. For this, we set our denominator equal to 0 and solve for β as a function of σ :

$$\beta = \frac{\mu_H c_1}{\alpha \left(1 + \frac{\gamma \rho \sigma}{c_2 c_3}\right)}. \quad (18)$$

After doing so, we plot β as a function of σ to obtain Figure 5.

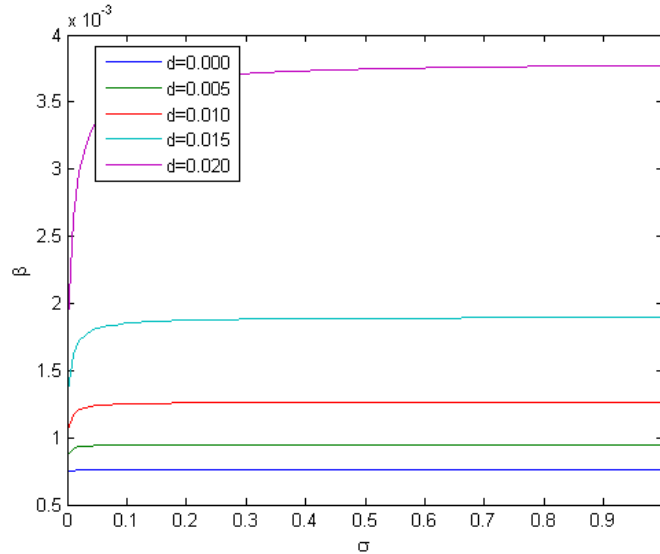


Figure 5: β vs σ , varying d , all other values fixed as in Table 1. Combinations of β and σ which lie below the curve produce a real H^* value for the given d value, while combinations on or above it do not. Corresponding β and σ values below the curve produce an asymptotically stable EE.

Only when $\beta < \left(\mu_H c_1 / \alpha \left(1 + \frac{\gamma \rho \sigma}{c_2 c_3}\right)\right)$ will H^* have biological relevance. Thus, in examining σ vs β , for any value of β and σ below the curve, H^* will exist. Hence, our equilibrium is present as long as the values of β and σ correspond to the area below the curve in σ vs β .

Similarly, when we fix β and vary σ and d , we find d as a function of σ to get the following:

$$d = \frac{\gamma \rho \sigma}{\left(\mu_j + \alpha\right) \left(-1 + \mu_H \frac{(\mu_j + \rho \sigma + \gamma)}{\beta \alpha}\right)} - \mu_j - \gamma. \quad (19)$$

Figure 6 demonstrates d as a function of σ .

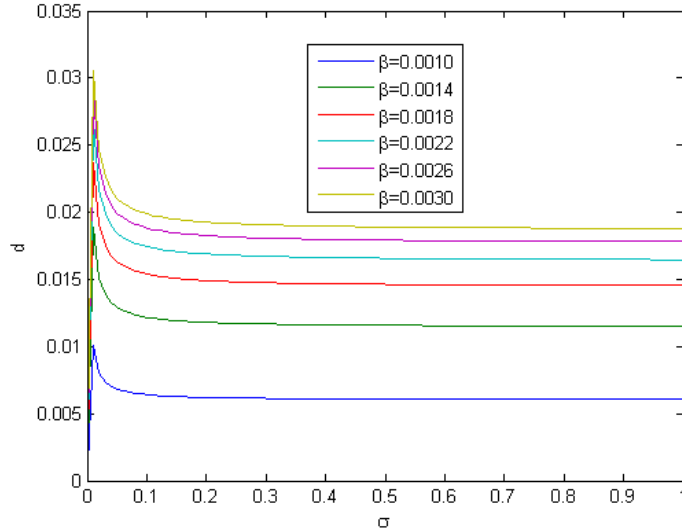


Figure 6: d vs σ , varying β . Combinations of d and σ which lie *above* the curve produce a real H^* value for the given β value, while combinations on or *below* it do not. Note that there is a vertical asymptote for each curve near $\sigma = 0$. Thus, for corresponding d and σ values below each curve, there exists an asymptotically stable EE.

An analogous analysis can be done for σ vs d : as long as the values of d and σ correspond to the area below the curve, then our equilibrium is of biological relevance.

Finally, as we fix σ and vary d and β , we get β as a function of d :

$$\beta = \frac{\mu_H(\mu_j + \rho\sigma + \gamma)(\mu_j + \alpha)(\mu_j + d + \gamma)}{\alpha(1 + \gamma\rho\sigma)}. \quad (20)$$

Figure 7 demonstrates the relationship between d and β .

As in the previous graphs, as long as d and β are such that they are below the curve in d vs β , then the equilibrium exists.

If we vary β , d , and σ all at once (see Figure 8), we obtain a surface such that, for any point in the area below the resulting surface corresponding to the values of β , d , and σ , the equilibrium exists.

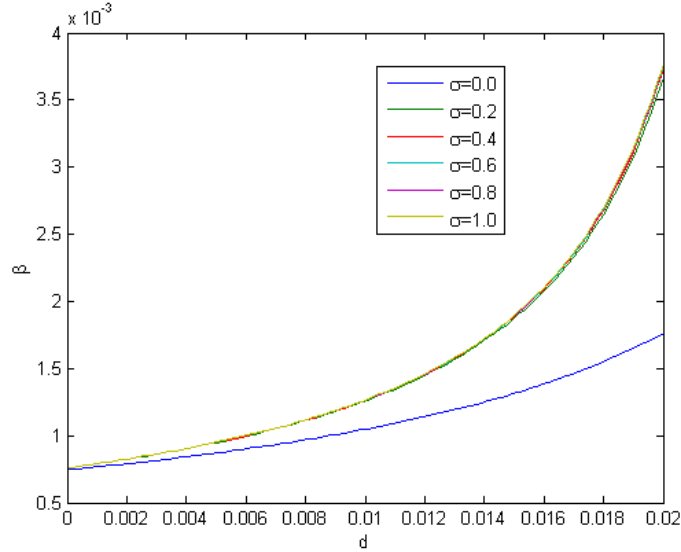


Figure 7: β vs d , varying σ . As in Figure 5, combinations of β and d which lie below the curve produce real H^* values for the given σ , while combinations on or above it do not. We can see clearly that only very low σ values appreciably affect our real H^* conditions.

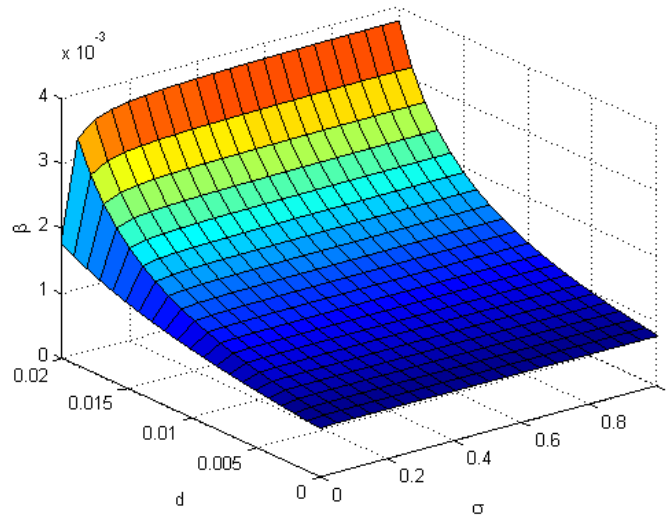


Figure 8: β vs d vs σ . This 3-dimensional plot combines the information from Figures 5, 6, and 7. Combinations of β , σ , and d which lie below the surface produce real H^* values, while combinations on or above it do not. The surface appears to have an extremely shallow slope in the σ dimension except for very low σ values, indicating that σ has relatively little impact on the existence of an equilibrium relative to β and d .

Knowing that σ does not affect the equilibrium (except for sufficiently small values), we study the birth rate, β , and the disease death rate, d . In Figure 9 we see that, for sufficiently small values of β and the rest of the parameters assuming their values in Table 1, the equilibrium (5)-(8) has biological relevance. Thus, the curve $H^*(\beta)$ is discontinuous when the denominator of (5) becomes 0. As for d , when we vary d while fixing the rest

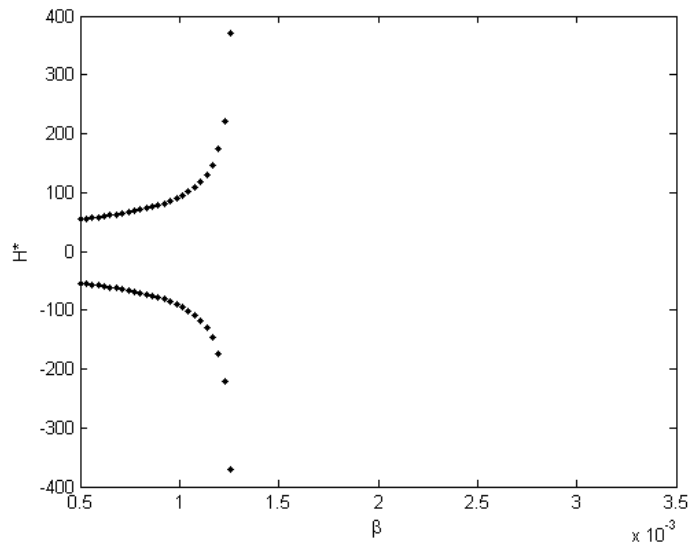


Figure 9: Bifurcation diagram of H^* vs β , with the rest of the parameters assuming values in Table 1. Here, we see that as the value of β increases, H^* ceases to exist. Only when β is sufficiently small does H^* have biological relevance.

of our parameters, our endemic equilibrium fails to exist when d is not sufficiently high. When d exceeds approximately $\frac{0.73}{40}$ (that is, when the proportion of columbids infected exceeds 0.72), we see that the endemic equilibrium becomes existent and also locally asymptotically stable.

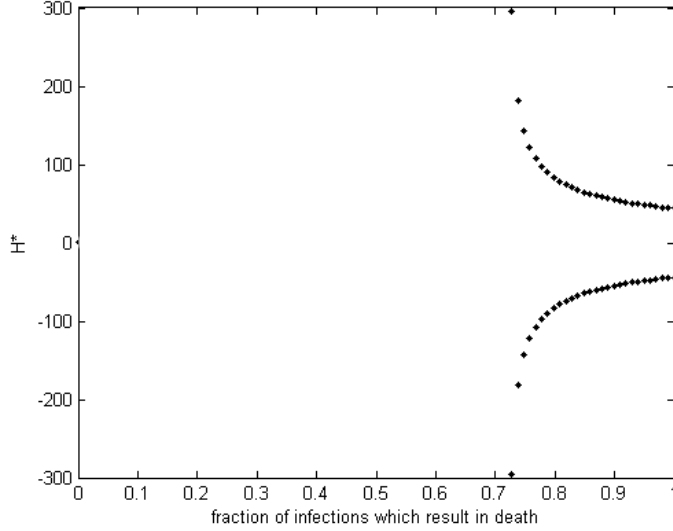


Figure 10: Bifurcation diagram of H^* vs d , with the rest of the parameters assuming values in Table 1. We see that, when the proportion of death due to infection is sufficiently low (i.e. when d assumes low enough values), H^* becomes non-existent. When this proportion is sufficiently large (≈ 0.72 or greater, or when $d > \frac{0.72}{40}$), then there exists an endemic equilibrium, which is locally asymptotically stable.

3 Stochastic model

3.1 Model Formulation

In addition to our deterministic system (1)-(4), we also constructed a stochastic model to capture the inherent variation of events happening in nature. This supplementary model takes the form of a continuous time Markov chain which simulates the changes in an urban Cooper’s hawk population for a set number of days, and is constructed based on the deterministic system (1)-(4).

The main difference between the two models is that the deterministic model is based on rates of flow between classes, while the stochastic model is based on probabilities of events. Hawks are able to enter, exit, and transfer between the H , S , I , and R classes in the same way as in the deterministic model (see Figure 1). Each of these transfers constitutes an event, and each event occurs at a certain rate, which depends on the current state of the system.

Table 2: Markov chain events and event rates. All of the rates are linear with the exception of the immigration rate.

Event	Outcome	Rate	Source
birth	$+1S$	βH	[35]
infection	$-1S, +1I$	$\rho\sigma S$	[26, 35, 42, 48]
recovery	$-1I, +1R$	γI	approx.
susceptible natural death	$-1S$	$\mu_j S$	[35]
infected natural death	$-1I$	$\mu_j I$	[35]
recovered natural death	$-1R$	$\mu_j R$	[35]
disease death	$-1I$	dI	[33]
susceptible aging	$+1H, -1S$	αS	[35]
recovered aging	$+1H, -1R$	αR	[35]
adult death	$-1H$	$\mu_H H$	approx.
immigration	$+1H$	Λ/H	approx.

We developed a program to model the hawk population through the following process (see Appendix D): Each possible event has a rate associated with it, given the current population in each hawk class. The various events and rates are described in Table 2. The parameters used in calculating these rates are numerically identical to those used in the deterministic model (see Table 1). While the parameters are in per capita terms, the fact that they are multiplied by the size of each class leaves us with total rates rather than per capita rates. We calculate the total rate of all events by adding all of the rates together. The probability of any particular event is that event's rate divided by the total event rate.

In order to determine which event occurs, we divide the space $[0, 1]$ into 11 segments. The size of each segment corresponds to the probability of each event, thus the sum of the sizes of the segments is 1. We then generate a uniform random variable in $[0, 1]$. The segment that it lies within determines which event occurs. Finally, we select the time at which the event occurs. Our stochastic model represents a Poisson process. The average time between the events is given by an exponential distribution. We calculate the time between each event by generating an exponential random variable whose mean parameter is the inverse of the total event rate. This process continues until a specified number of days has elapsed. The final output of our program is a series of event times and corresponding class sizes for each time.

Unlike the deterministic model, our stochastic model could not be evaluated analytically. Instead, we ran the simulation many times and conducted statistical analysis on the outcome of the suite of realizations. Results of these simulations will be given in Section 3.2. We began by running simulations using the parameters from our research, and eventually began to vary our values of σ , β , and d to measure their effects on the annual

population growth rate.

3.2 Extension of Stochastic Model

In addition to our stochastic model based directly on our system of ODEs, we also constructed an extension of this stochastic model in an attempt to add as much realism as possible. It differs from our first stochastic model in a number of significant ways. For one, we separate hawks into the following eight classes, rather than only four:

Mating adult hawks have reached sexual maturity and reproduce during the nesting season.

Non-mating adult hawks have reached sexual maturity but do not reproduce during the current mating season.

2nd year fledgelings will reach sexual maturity and be able to reproduce during the following nesting season.

1st year fledgelings have left their nest, but will not be able to reproduce for two more nesting seasons.

Susceptible nestlings still receive food from their parents, and may contract the disease if fed infected food.

Latent nestlings have contracted the disease, but it has not yet progressed far enough to contribute to their death rate.

Infected nestlings have had the disease for a while, and as a result have a significantly higher death rate than other nestlings.

Recovered nestlings have had the disease long enough that their immune system is able to protect them from its detrimental effects.

As with the first model, hawks are able to enter, exit, and transfer between these various classes through a number of processes. Unlike the Markov chain model, however, which essentially represents a completely homogeneous timeframe with no seasonal effects, this new model takes into account a discrete, annual nesting season. The other major difference is in the way that events are evaluated. The Markov chain model takes place in continuous time, with one event occurring at a time. This new model takes place in discrete time divided by days. Rather than determining which type of event occurs by calculating the probability of each type, we run through each hawk individually to determine whether various events occur for them. We developed a program to run a daily process for each of the hawk classes. Which processes are conducted depends on whether or not the nesting season is in progress.

The process begins with a specified number of initial adult hawks and 2nd year fledgelings at the beginning of the nesting season. For simplicity, we assume that only adult hawks reproduce, that they all reproduce at the same time, and that sex ratios are never an issue in terms of mating. First we sort the adult population into a mating portion and a non-mating portion. This is accomplished through use of a uniform random variable, with each hawk having a 0.66 chance of being placed in the mating portion. If the mating portion turns out to be an odd number, one hawk is transferred to the non-mating group. We then pair the mating adults and assign each pair to a nest. Nests are kept track of separately in the simulation. We assign each nest a normally distributed random number of hatchlings with a mean of 3.44 and a standard deviation of 1.02 [35], mapping negative outcomes to zero. Hatchlings are placed directly into the susceptible class.

Next we go through the nesting period, which lasts for 40 days. We use this number since it is the age at which the hawks' immune systems are assumed to be developed enough to fight off the infection [35]. Since infections are spread exclusively through feeding, the main daily simulation process uses a series of nested loops to determine new infections due to consumption of infected columbids. Each day we go through each nest, one-by-one. For each nest we determine the number of prey items brought in, which is a normally distributed random variable with a mean of 8.9 and a standard deviation of 1.5 [42], again mapping negative outcomes to zero. For each prey item, we determine the chance that it happens to be an infected columbid using the uniform random variable method from the previous model. If it is infected, we go through each susceptible nestling to determine the chance that it contracts the infection. If the nestling contracts the disease, it is moved from the susceptible to the latent class.

Next we evaluate the daily infection progression. Unlike the previous two models, our stochastic model includes a latent class to represent the fact that the infection takes time to become deadly to a nestling. We assume that it takes approximately 7 days for the disease to become deadly, and that it kills infected nestlings for approximately 14 days after that. To model this, every day each latent hawk has a $1/7$ chance to move into the infected class, and each infected hawk has a $0.59/14$ chance to move into the recovered class (since 41% of them die within that period). On average, this should cause surviving hawks to spend 7 days in the latent class and 14 days in the infected class.

Finally, we evaluate the daily mortality and immigration. Adults, fledgelings, and nestlings all have a corresponding natural mortality rate, which represents their probability of dying due to natural causes every day. We go through every single hawk in the population and use a random uniform variable to determine whether it dies. Infected nestlings have a higher probability of dying than other nestlings. There is also a small chance that a number of adult hawks immigrate into the system. Since the nesting period is already in progress if and when this happens, any new immigrants are deposited directly into the non-mating adult population.

At the end of the nesting period, we assume that all nestlings have a robust enough immune system that they are safe from the disease. Regardless of which nestling class they are currently in, they are all promoted to 1st year fledgelings. This begins the non-nesting

period, which is much simpler to simulate. Since new infections no longer contribute to the death rate of the hawks, we do not consider feeding habits. The only things which occur during the non-nesting period are natural deaths and immigrations. They are evaluated in the same way as before, with a distinct mortality rate for each of the three fledgeling classes.

The end of the year signifies the beginning of a new nesting season. When we reach this point, each of the fledgeling classes is promoted by one year. 2nd year fledgelings can now mate, and are moved to the adult class. 1st year fledgelings become 2nd year fledgelings, and will be able to mate next year. We once again isolate the mating portion of the adult population, assign them to nests, generate a random number of births for each nest, and repeat the process over again. The simulation continues to go through the nesting and non-nesting portions of the year until the predetermined number of days has expired.

This simulation depends on a large number of parameter values, which were chosen through a combination of research and trial and error in an effort to get the model to achieve realistic behavior. They are summarized in Table 3.

Table 3: Parameters' definitions and values, stochastic model 2

Parameter	Definition	Value	Source
doveprob	Probability that prey item is a dove	0.83	[33]
idoveprob	Probability that any given dove is infected	0.423	[26]
nestdays	Age (days) at which hawks become immune to the disease	40	[35]
ichance	Probability of becoming infected from eating an infected dove	1/30	[48]
muH	Daily probability of an adult hawk dying naturally	1/(365·5)	approx.
muHy2	Daily probability of a 2nd year fledgling dying naturally	0.31/365	[35]
muHy1	Daily probability of a 1st year fledgling dying naturally	0.31/365	[35]
muY	Daily probability of a nestling dying naturally	0.36/40	[33]
d	Daily probability of an infected nestling dying from disease	0.41/14	[33]
latency	Daily probability of becoming infected if latent	1/7	approx.
iperiod	Daily probability of recovering if infected	0.59/14	[33]
avgeggs	Average hatchlings per nest	3.44	[35]
stdeveggs	Standard deviation of hatchlings per nest	1.02	[35]
avgfood	Average prey items per nest per day	8.9	[42]
stdevfood	Standard deviation of prey items per nest per day	1.5	[42]
matefrac	Fraction of adults that actually produce nests	2/3	approx.
lambda	Immigration rate	1	approx.

The program also reports a number of important statistics upon its completion. Our analysis of this model was completed by running the simulation for 1000 realizations at 10 years per realization and averaging the results of each. In particular we were interested in the annual growth rate produced by this model.

3.3 Results

We begin by running our Markov chain model for 1000 realizations for 10 simulated years per realization. For each realization we acquired the total number of each event type as well as the average annual growth rate. Across the 1000 realizations we came up with an average annual growth rate of 15.8%, with a standard deviation of 0.902%. As expected, this supports the claim that the hawk population in Tuscon is currently increasing.

After testing our real-world parameters, we moved on to testing variations. For the following figures we varied each parameter, β , σ , and d , and ran our Markov chain model 250 times. We then measured the average population growth rate of each run for each varying parameter. Each data point in the figures represents the average population growth rate for each parameter varied. For Figures 11-13 we fix the parameters from Table 1.

In Figure 11, as we increase β , we notice that the average annual population growth linearly increases. Only at very low β values do we see nonpositive population growth.

In Figure 12, σ is varied while the rest of parameters are fixed. We see that, as σ approaches 0, the population growth rate greatly increases. As σ increases, however, the population growth rate decreases, asymptotically reaching a positive value. This demonstrates that, regardless of the value of σ is, the hawk population will not die out with our current parameters.

In Figure 13, we vary d as we fix the rest of our parameters. Figure 13 indicates that there is a linearly decreasing relation between the disease rate and the population growth rate: as the disease rate increases, the adult hawk population decreases. If the disease death rate, d , is large enough, then the population growth will become nonpositive. In fact, d is greater than or equal to $\frac{0.74}{40}$ (which reduces the recovery rate, γ , to $\frac{0.24}{40}$ or less), then our endemic equilibrium exists and is locally asymptotically stable.

3.4 Extension of Stochastic Model

Despite our best efforts to implement the most realistic set of parameters possible, we were unable to achieve sufficiently realistic behavior from our alternate stochastic model. For this reason, we ignored it in the evaluation of our research question. After running the simulation 1000 times with our standard parameters, the average annual population growth rate was -10.8%, indicating overall population decline. This conflicts with our real-world estimate of the hawk population growth in Tuscon of $\approx 11\%$ [35]. Figures 15 and 16 display the basic behavior of the model in two different ways.

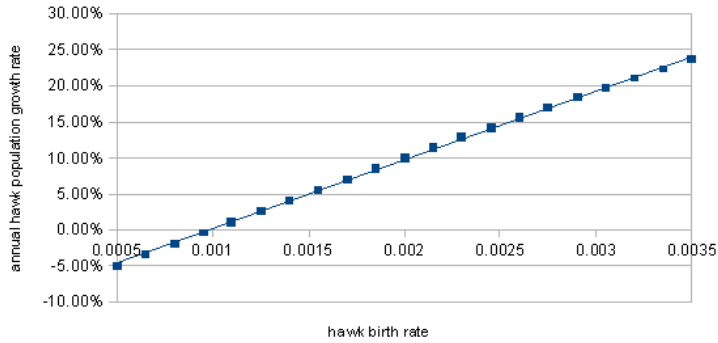


Figure 11: Hawk population growth rate as a function of β . Each point represents the average population growth rate after 250 realizations for the corresponding β value. β appears to have a positive linear relationship with the growth rate, illustrated by the included regression line (which has $R^2 > 0.999$).

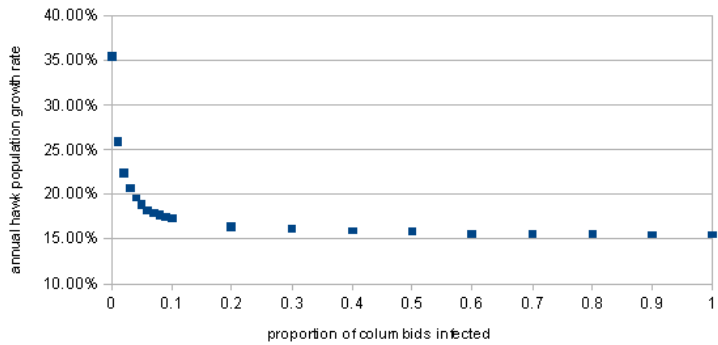


Figure 12: Hawk population growth rate as a function of σ . Each point represents the average population growth rate after 250 realizations for the corresponding σ value. σ appears to have a negative relationship with the growth rate, but approaches a horizontal asymptote. As σ increases, each increment has less of an impact on the population growth than the last.

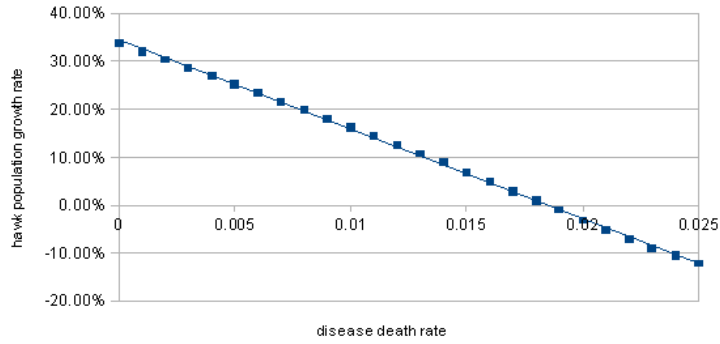


Figure 13: Hawk population growth rate as a function of d . Each point represents the average population growth rate after 250 realizations for the corresponding d value. d appears to have a negative linear relationship with the growth rate, as illustrated by the included regression line (which has $R^2 > 0.999$).

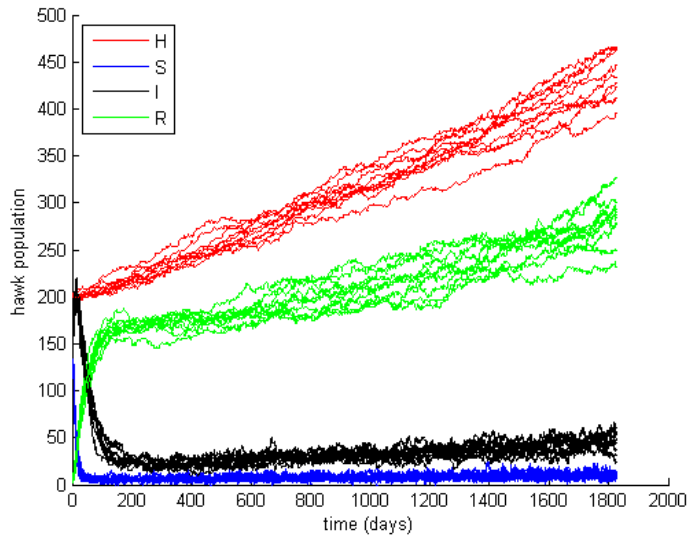


Figure 14: 10 realizations with Markov chain model with four classes of hawks. Parameter values may be found in Table 1. This figure is the stochastic analog of Figure 2.

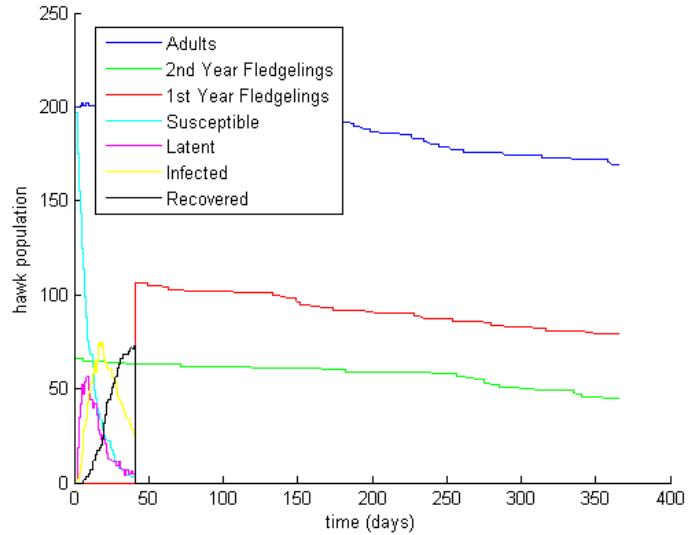


Figure 15: 1 year of simulation with the alternate stochastic model. The different lines track the various hawk classes. The sharp divide at the 40 day mark represents the point at which the nestling classes are emptied into the 1st year fledgeling class.

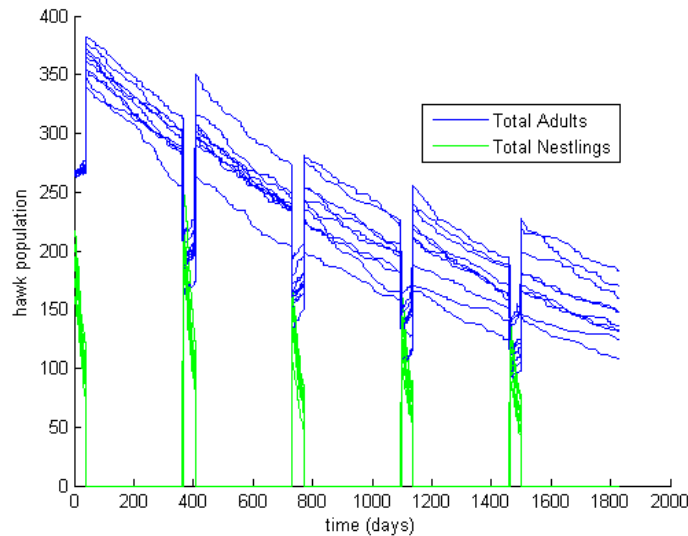


Figure 16: 10 realizations of the alternate stochastic model, each simulating 5 years. The adults and the two fledgeling classes are grouped together for this graph, as are the four nestling classes which exist only during the nesting season. Although the overall population rises and falls due to the punctuated birth events, there is an overall annual population decline. Due to this overall population decline, we thus chose to address our research question with the deterministic and simpler stochastic models.

4 Discussion

The results from our deterministic and four-class stochastic model both support the same results: there is no way for the infection rate in the columbids to ever become high enough to cause the Cooper's hawk population to decline even without immigration. This can be seen in Figures 2, 14 that after a year the hawk population would tend to grow exponentially and as it grows the immigration rate approximates the value of zero. Moreover, the results displayed in Figure 12 indicate that an increase in σ from its current value would not likely cause any appreciable impact in the hawk population, whatsoever. Only a drastic increase in the disease's virulence, as noted in Figure 13, or a drastic change in the hawks' life histories (i.e. a decrease in birth rate), as demonstrated by Figure 11, would negatively affect their population. It should be noted, however, that very low values of σ could still affect the hawk population, albeit in a positive way. This can be seen from Figures 5, 6, and 10, in which only very small σ values produce a significant change in the real H^* boundary.

Figures 11 and 13 demonstrate that both β and d have a linear relationship with population growth. After linear regression, both produce $R^2 > 0.999$. We used linear regression to quantify the point at which each would cause negative population growth. In the case of the birth rate, $\beta < 0.000985$ (37% of the current birth rate) would cause a population decrease. In the case of disease death rate, $d > 0.0185$ (180% of the current disease death rate, corresponding to 74.0% of infections resulting in death), would cause a population decrease.

5 Conclusion

As detailed in the Results subsection in Sections 2 and 3, given the current hatchling, infection and transmission rates, Table 1, there is never an EE within the Cooper's Hawk population and the population grows exponentially. Thus, even if all the columbids were infected with *T. gallinae* the hawk population would not decline even without immigration. We found that the disease death rate would have to be greater than 74.0%, or the hatchling rate to be less than 37% of its current value in order for the population to go into decline, also meaning that the EE will become stable given one of the changes mentioned to the parameters. Our EE,(5)-(8), can only exist being stable, because the Routh-Hurwitz Criterion for stability in our system,(1)-(4), depends on (9) holding and if this inequality does not hold there cannot be a decline or stability in the hawks population growth.

Our original research question was whether there was any way for the disease prevalence within the Tucson columbid population to rise high enough to create an ecological trap for the Cooper's hawk. The answer to that question, according to our model, is that infection rate, alone, would not be enough to create such a trap. On the other hand, we discovered that Tucson *could* become an ecological trap if a particularly virulent strain entered the hawk population and increased the disease death rate to over 180% of its

current value. However, this classification as an ecological trap only holds true if the columbid populations remain primarily asymptomatic carriers of the disease and their numbers do not decrease.

Our results confirm Boal's 2008 findings that the growth rate of the population is greater than one. Our stochastic model determined it to be 15.8% as opposed to 11%; thus the population may be growing faster than he claims.

Future research may include investigating the immune system of the nestling hawks to determine the nature of their immunity to the parasite. To date this has not been fully explored. We question whether it is the immune system that becomes fully functioning and thus the hawks are able to resist the parasite or if exposure to it early in life acts as a vaccination against the parasite later in life. Also, we could further develop the more complex stochastic model to more closely mirror the status of the current population.

Current phylogenetic analysis of *T. gallinae* indicates there is a strain endemic to the southwestern US that is not found in other parts [43, 44]. Future research could include testing samples of the parasite from Cooper's hawks to see if this strain is present in the Tucson population. This would explain the difference in prevalence rates between this population and those found in the midwestern US [33, 46].

6 Acknowledgements

Foremost, we would like to thank Carlos Castillo-Chavez, Executive Director of the Mathematical and Theoretical Biological Institute, for giving us the opportunity to participate in this research program. A special thanks is also given to our mentors Jose Vega, Susan Holechek, Erika Camacho, Ben Morin, David Murillo, Baojun Song, and Karen Rios-Soto for all their insight and support. Further special thanks go to Preston Swan, Liberty Wildlife, and Wendy. This research was conducted in the Mathematical and Theoretical Biology Institute (MTBI) at the Mathematical, Computational and Modeling Sciences Center (MCMSC). This project has been partially supported by grants from the National Science Foundation (NSF - Grant DMP-0838705), the National Security Agency (NSA - Grant H98230-11-1-0211), the Alfred P. Sloan Foundation and the Office of the Provost of Arizona State University. The Mathematical and Theoretical Biology Institute, now hosted at the Mathematical, Computational and Modeling Science Center at ASU, would like to give thanks to everybody involved with the program for the past 16 years.

References

- [1] Dwernychuk, L. W., and D. A. Boag. *Ducks nesting in association with gulls: an ecological trap?* Canadian Journal of Zoology, **50** (1972), 559-563.
- [2] Delibes, M., Goana, P. F. *Effects of an attractive sink leading into maladaptive habitat selection.* Am. Naturalist, **158** (2001), 277-285.

- [3] Schlaepfer, M. A., Runge, M. C., Sherman, P.W., *Ecological and evolutionary traps*. *TRENDS in Ecology & Evolution*, **17** (2002), pp. 474-480.
- [4] Gilroy, J. J., Sutherland, W. J. *Beyond ecological traps: perceptual errors and undervalued resources*, *TRENDS in Ecology and Evolution*, **22** (2007), pp. 351-356.
- [5] Battin, J. *When good animals love bad habitats: Ecological traps and the conservation of animal populations*, *Conservation Biology*, **18** (2004), pp. 1482-1491.
- [6] Robertson, B. A. and Hutto, R. L., *A framework for understanding ecological traps and an evaluation of existing evidence*, *Ecology*, **87** (2006) pp. 1075-1085.
- [7] Robertson, B., Kriska, G., Horvath, V. and Horvath, G. *Glass buildings as bird feeders: urban birds exploit insects trapped by polarized light pollution*. *Acta Zoologica Academiae Scientiarum Hungaricae*, **56** (2010) pp.283-293.
- [8] Kriska, G. et al., *Glass buildings on river banks as "polarized light traps" for mass-swarming phototactic caddis flies*, *Naturwissenschaften*, **95** (2008), pp. 461-467.
- [9] DeMara, B., *Lights take toll on birds*, *Toronto Star* April 8, 2005, pp. B03.
- [10] Sibley, D. A. *Window pain*, *Birder's World*, December 2008, pp. 34.
- [11] Mac Nally, R. *Ecological boundary detection using Carlin-Chib Bayesian model selection*, *Diversity and Distributions*, **11** (2005) pp. 499-508.
- [12] Fortin M. *Detection of ecotones: definition and scaling factors*. PhD. dissertation, State Univ. of NY at Stony Brook, (1992).
- [13] Dangerfield, J. M., Pik, A. J., Britton, D. et al. *Patterns of invertebrate biodiversity across a natural edge*, *Austral Ecology*, **28** (2003) pp. 227-236.
- [14] Weldon, A. J., *How corridors reduce indigo bunting nest success*, *Conservation Biology*, **29** (2006) pp. 1300-1305.
- [15] Weldon, A.J. and Haddad, N, *The effects of patch shape on Indigo buntings: Evidence for an ecological trap*, *Ecology* **86**(2005), pp 1422-1431.
- [16] Zugmeyer, C.A., Koprowski, J.L., *Severely insect-damaged forest: A temporary trap for red squirrels?*, *Forest Ecol. and Mangmt.* **2**, (2009), pp 464-470.
- [17] Igual, J.M., Forero, M.G., Gomez, T., and Oro, D. *Can an introduced predator trigger and evolutionary trap in a colonial seabird?*, *Biological Conservation* **137** (2007), pp. 189-196.
- [18] Gates, J. E. and Gysel, L. W., *Avian nest dispersion and fledging success in field-forest ecotones*, *Ecology*, **59** (1978), pp. 871-883.

- [19] Brooks, T. M., Mittermeier, R. A., DA Fonseca, G. A. B., et al. *Habitat loss and extinction in the hotspots of biodiversity*, Conservation Biology, **16** (2001) pp. 909-923.
- [20] Sang, A. Teder, T. Helm, A., and Partel, M. *Indirect evidence for an extinction debt of grassland butterflies half a century after habitat loss*, Biological Conservation, **143** (2010) pp. 1405-1413.
- [21] Mannan, R. W., *Exurban land development and breeding birds*, The Planner's Guide to Natural Resource Conservation. Springer Science + Bus. Media, LLC (2009).
- [22] Young, E., *Evaluating and monitoring habitat loss sing remote sensing imagery* M.Sc. Thesis, University of Ottawa (2009).
- [23] Worden, M. A., and Kok, D. A. *Population growth in Arizona*, Economic Development Journal, **6** (2007) pp. 18-25.
- [24] Brown, D. E., *Arizona Game Birds*, University of Arizona Press (1989) pp. 253.
- [25] Germaine, S. S., *Realationshipes of birds, lizards, and nocturnal rodents to their habitat in the greater Tucson, Arizona*, Ariz. Game and Fish Dept. Tech. Rep. 20.
- [26] Hedlund, C. A., *Trichomonas gallinae in avian populations in urban Tucson, Arizona*, MS Thesis, University of Arizona (1998).
- [27] Holeyvinski, R. A., Malecki, R. A., and Curtis, P. D. *Can hunting of translocated Canada Geese reduce local conflicts?*, Wildlife Soc. Bull., **34** (2006) pp. 845-849.
- [28] Blewett, C. M., and Marzluff, J. M., *Effects of urban sprawl on snags and the abundance and productivity of cavity-nesting birds*, The Condor, **107** (2005) pp 678-693.
- [29] Ticer, C. L., Ockenfels, R. A., and Devos, J. C., *Habitat use and activity patterns of urban-dwelling javelina*, Urban Ecosystems, **2** (1998), pp. 141-151.
- [30] Shaw, J. C., Neural mechanisms of behavior modifaictation in killifish (*Funfulus parvipinnis*) by a brain parasite (*Euhaplochis californiensis*) and the ecology of the host-parasite relationship. Dissertation (2007) University of California, Santa Barbara.
- [31] Manga-Gonzalez, M.Y., Gonzalez-Lanza, C., et al. *Contributions to and review of dicrocoeliosis, with special reference to the intermediate hosts of Dicrocoelium dendriticum*, Parasitology **123** (2001), pp. S9-S114.
- [32] Berdoy, M., Webster, J.P., MacDonald, D. W., *Fatal attraction in rats infected with Toxoplasma gondii*, Proc. R. Soc. Lond. B. **267**, (2000), 1591-1594.

- [33] Boal, C.W., *An urban environment as an ecological trap for Cooper's hawks*, Phd. Dissertation, University of Arizona (1997).
- [34] Boal, C. W., Mannan, R. W. and Hudelson, K. S., *Trichomoniasis in Cooper's hawks from Arizona*, Journal of Wildlife Diseases, **34** (1998), pp. 590-593s
- [35] Boal, C. W., Mannan, R. W. and Steidl, R. J., *Identifying habitat sinks: a case study of Cooper's hawks in an urban environment*, Urban Ecosyst, **11** (2008), pp. 141-148.
- [36] Boal, C. W., and Mannan, R. W., *Breeding ecology of Cooper's hawks in urban and exurban areas of southeastern Arizona*, Jour. Wldlfe Mang. **63** (1999) pp. 77-84
- [37] Mannan, R. W., and Boal, C. W., *Home range characteristics of male Cooper's hawks in and urban environment*, The Wilson Bulletin **112** (2000), pp 21-27.
- [38] Boal, C. W., and Mannan, R. W., *Cooper's hawks in urban and exurban areas: a reply*, Jour. Wldlfe Mang. **64** (2000) pp. 601-604.
- [39] Boal, C. W., *Nonrandom mating and productivity of adult and subadult Cooper's hawks*, The Condor **103** (2001), pp 381-385.
- [40] Mannan, R.W., Mannan, R.N., Schmidt, C.A. et al. *Influence of natal experience on nest-site selection by urban-nesting Cooper's hawks*, Journ. Wldlf. Mangmt., **71** (2007), pp. 64-68.
- [41] Straus, M. A., *Incidence of Trichomonas gallinae in Mourning Dove, Zenaidura macroura, populations of Arizona*. MS thesis, University of Arizona (1966).
- [42] Estes, W. A. and Mannan, R. W., *Feeding behavior of Cooper's hawks at urban and rural nests in southeastern Arizona*, The Condor, **105** (2003), pp. 107-116.
- [43] Feiler, A. L., *Phylogenetic analysis of Trichomonas complex*, Unpublished research (2010).
- [44] Gerhold, G. W., Yabsley, M. J., et al. *Molecular characterization of the Trichomonas gallinae morphologic complex in the United States*, Journal of Parasitology, **94** (2008), pp. 1335-1341.
- [45] Rosenfield, R. N. et al., *Prevalence of Trichomonas gallinae in nestling Coopers hawks among three North American populations*, Wilson Bulletin, **114**(2002), pp. 145-147
- [46] Rosenfield, R. N., Taft, S. J., et al., *Low prevalence of Trichomonas gallinae in urban and migratory Coopers hawks in north central North America*. The Wilson Journal of Ornithology, **121** (2009), pp. 641-644.
- [47] Sileo, L., and Fitzhugh, E. L., *Incidence of trichomoniasis in the band-tailed pigeons of southern Arizona*. Bulletin of the Wildlife Disease Association, **5** (1969), pp. 146.

- [48] Stabler, R.M., *Further studies on trichomoniasis in birds*. The Auk, 58 (1941), pp. 558-562.
- [49] Stabler, R. M., *A survey of Band-tailed pigeons, mourning doves and wild common pigeons for Trichomonas gallinae*, The Journal of Parasitology, **37** (1951), pp. 471-472.
- [50] Stamps, J. and Krishnan, V. V., *Nonintuitive Cue Use Habitat Selection*. Ecology, 86 (2005), pp. 2860-2867.
- [51] Stephens, R.M., Anderson, S.H., *Conservation assessment for the Cooper's hawk and Sharp-shinned hawk in the Black Hills National Forest, South Dakota and Wyoming* Wyoming Coop. Fish and Wldlf. Unit, Univeristy of Wyoming.

Appendix

A Process for finding the endemic equilibrium

Set \dot{H} , \dot{S} , \dot{I} , and \dot{R} in (1)-(4) to 0 as follows:

$$0 = \alpha(S + R) - \mu_H H + \frac{\Lambda}{H}, \quad (21)$$

$$0 = \beta H - (\rho\sigma + \mu_j + \alpha)S, \quad (22)$$

$$0 = \rho\sigma S - (\mu_j + d + \gamma)I, \quad (23)$$

$$0 = \gamma I - (\mu_j + \alpha)R. \quad (24)$$

In working with (22), we will solve for S in terms of H :

$$(\rho\sigma + \mu_j + \alpha)S = \beta H \implies S = \frac{\beta H}{\rho\sigma + \mu_j + \alpha}. \quad (25)$$

For (23), we solve for I :

$$\rho\sigma S = (\mu_j + d + \gamma)I \implies I = \frac{\rho\sigma S}{\mu_j + d + \gamma}. \quad (26)$$

Similarly, for (24), R will be solved in terms of I :

$$(\mu_j + \alpha)R = \gamma I \implies R = \frac{\gamma I}{\mu_j + \alpha}. \quad (27)$$

By (26), R can be rewritten in terms of S in (26):

$$R = \frac{\gamma\rho\sigma S}{(\mu_j + \alpha)(\mu_j + d + \gamma)}. \quad (28)$$

Thus, by (28) and (25), (21) can be written as follows:

$$0 = \alpha \left(1 + \frac{\gamma\rho\sigma}{(\mu_j + \alpha)(\mu_j + d + \gamma)} \right) S - \mu_H H + \frac{\Lambda}{H}. \quad (29)$$

By (25), S can be written in terms of H . thus, (29) is rewritten as:

$$0 = \left(1 + \frac{\gamma\rho\sigma}{(\mu_j + \alpha)(\mu_j + d + \gamma)} \right) \left(\frac{\beta}{\rho\sigma + \mu_j + \alpha} \right) H - \mu_H H + \frac{\Lambda}{H}. \quad (30)$$

Now we can solely solve for H . Dividing by H on both sides for (30), we get the following:

$$0 = \left(1 + \frac{\gamma\rho\sigma}{(\mu_j + \alpha)(\mu_j + d + \gamma)}\right) \left(\frac{\beta}{\rho\sigma + \mu_j + \alpha}\right) - \mu_H + \frac{\Lambda}{H^2}. \quad (31)$$

As we isolate and solve for H , we wish to take the positive square root of H rather than the negative value since we are concerned with a biologically relevant equilibrium. Doing so, we get the following:

$$H^* = \left(\frac{\Lambda}{\mu_H - \left(1 + \frac{\gamma\rho\sigma}{(\mu_j + \alpha)(\mu_j + d + \gamma)}\right) \left(\frac{\beta}{\rho\sigma + \mu_j + \alpha}\right)}\right)^{\frac{1}{2}}. \quad (32)$$

We then make the following simplifications to our parameters:

$$c_1 = \rho\sigma + \mu_j + \alpha, \quad c_2 = \mu_j + d + \alpha, \quad c_3 = \mu_j + \alpha \quad (33)$$

Substituting (33) onto (32), we then get the following value as part of our equilibrium:

$$H^* = \left(\frac{\Lambda}{\mu_H - \left(1 + \frac{\gamma\rho\sigma}{c_3c_2}\right) \left(\frac{\beta}{c_1}\right)}\right)^{\frac{1}{2}}. \quad (34)$$

This can be rewritten into the following:

$$H^* = \left(\frac{\Lambda c_1 c_2 c_3}{\mu_H c_1 c_2 c_3 - \beta \alpha (c_2 c_3 + \gamma \rho \sigma)}\right)^{\frac{1}{2}}. \quad (35)$$

As has been noted before, this value will always be positive as long as $\frac{\beta \theta \alpha (c_2 c_3 + \gamma \rho \sigma)}{c_1 c_2 c_3} < \mu_H$. We insert H^* into (31) to find our corresponding S^* for our equilibrium:

$$S^* = \frac{\beta H^*}{\mu_j + \rho\sigma + \alpha}. \quad (36)$$

Finally, substituting (36) into (26) and (27) will result in finding I^* and R^* :

$$I^* = \frac{\beta \rho \sigma H^*}{(\mu_j + d_j + \gamma)(\mu_j + \rho\sigma + \alpha)}, \quad (37)$$

$$R^* = \frac{\gamma \beta \rho \sigma H^*}{(\mu_j + \alpha)(\mu_j + d_j + \gamma)(\mu_j + \rho\sigma + \alpha)}. \quad (38)$$

Since our parameters are all positive, H^* , S^* , I^* , and R^* will remain positive, and will be biologically relevant.

Hence, our endemic equilibrium is give by:

$$\begin{aligned}
H^* &= \left(\frac{\Lambda}{\mu_H - \left(1 + \frac{\gamma\rho\sigma}{(\mu_j + \alpha)(\mu_j + d + \gamma)}\right) \left(\frac{\beta}{\rho\sigma + \mu_j + \alpha}\right)} \right)^{\frac{1}{2}}, \\
S^* &= \frac{\beta H^*}{\mu_j + \rho\sigma + \alpha}, \\
I^* &= \frac{\beta\rho\sigma H^*}{(\mu_j + d_j + \gamma)(\mu_j + \rho\sigma + \alpha)}, \\
R^* &= \frac{\gamma\beta\rho\sigma H^*}{(\mu_j + \alpha)(\mu_j + d_j + \gamma)(\mu_j + \rho\sigma + \alpha)}.
\end{aligned}$$

B Inequality Conditions

First, we will assume the endemic equilibrium is biologically relevant and thus assume following is true:

$$\frac{\beta\alpha(c_2c_3 + \gamma\rho\sigma)}{c_1c_2c_3} < \mu_H. \quad (39)$$

We will also assume our simplifications from earlier:

$$\begin{aligned}
c_1 &= \rho\sigma + \mu_j + \alpha, & c_2 &= \mu_j + d + \alpha, & c_3 &= \mu_j + \alpha, \\
A &= -2\mu_H + \frac{\beta\alpha(c_2c_3 + \gamma\rho\sigma)}{c_1c_2c_3}.
\end{aligned} \quad (40)$$

With the assumption that all our parameters are positive, we see that c_1 , c_2 , and c_3 are positive.

Since (39) implies that $\frac{\beta\alpha(c_2c_3 + \gamma\rho\sigma)}{c_1c_2c_3} - \mu_H < 0$, this means that $A < 0$. Thus, $-A > 0$.

Let us equate a_{n_i} to the following coefficients for $n_i \in \{1, 2, 3, 4\}$:

$$\begin{aligned}
a_1 &= c_1 + c_2 + c_3 - A, & a_2 &= c_1c_2 + c_2c_3 + c_1c_3 - (c_1 + c_2 + c_3)A - \beta\alpha, \\
a_3 &= (c_1c_2c_3 - (c_1c_2 + c_2c_3 + c_1c_3)A - \beta\alpha(c_2 + c_3)), & a_4 &= -(c_1c_2c_3A + \beta\alpha c_2c_3 + \beta\rho\sigma\alpha\gamma).
\end{aligned}$$

For our endemic equilibrium to satisfy the Routh-Hurwitz criterion, we first wish to show that a_1, a_3 , and a_4 are positive. Since c_1, c_2, c_3 , and $-A$ are greater than 0, we have a_1 being positive.

For a_3 , we have the following:

$$a_3 = c_1 c_2 c_3 - (c_1 c_2 + c_2 c_3 + c_2 c_3)A - \beta \alpha (c_2 + c_3) \quad (41)$$

$$= c_1 c_2 c_3 - c_2 c_3 A - (c_2 + c_3)c_1 A - (c_2 + c_3)\beta \theta \alpha \quad (42)$$

$$> -(c_2 + c_3)(c_1 A + \beta \alpha). \quad (43)$$

To show that (42) is positive, it is sufficient to show that $c_1 A + \beta \alpha < 0$, as c_2 and c_3 are already positive. Thus, we have:

$$c_1 A + \beta \alpha = \beta \alpha \left(\frac{c_1 A}{\beta \alpha} + 1 \right). \quad (44)$$

By (39), we have:

$$2\mu_H > \frac{2\alpha\beta}{c_1} \left(1 + \frac{\gamma\rho\sigma}{c_2 c_3} \right) \quad (45)$$

$$\implies -2\mu_H < \frac{2\alpha\beta\theta}{c_1} \left(1 + \frac{\gamma\rho\sigma}{c_2 c_3} \right). \quad (46)$$

Now we will show that $\frac{c_1 A}{\beta \alpha} + 1 < 0$. From (40), we now have:

$$\frac{c_1 A}{\beta \alpha} + 1 = \frac{c_1}{\beta \alpha} \left(-2\mu_H + \frac{\beta \alpha (c_2 c_3 + \gamma \rho \sigma)}{c_1 c_2 c_3} \right) + 1 \quad (47)$$

$$< \frac{c_1}{\beta \alpha} \left(\frac{-2\alpha\beta}{c_1} \left(1 + \frac{\gamma\rho\sigma}{c_2 c_3} \right) + \frac{\alpha\beta(c_2 c_3 + \gamma\rho\sigma)}{c_1 c_2 c_3} \right) + 1 \quad (48)$$

$$= \frac{-c_2 c_3 + \gamma \rho \sigma}{c_2 c_3} + 1 \quad (49)$$

$$= -1 - \frac{\gamma \rho \sigma}{c_2 c_3} + 1 \quad (50)$$

$$= -\frac{\gamma \rho \sigma}{c_2 c_3} \quad (51)$$

$$< 0. \quad (52)$$

Hence, a_3 is positive.

For a_4 , upon substituting A in terms of our parameters, we see that a_4 is rewritten as:

$$a_4 = 2(\mu c_1 c_2 c_3 - \beta \alpha (c_2 c_3 + \rho \sigma \gamma)). \quad (53)$$

By (38), a_4 is positive.

For the final inequality of the Routh-Hurwitz criterion, $a_1 a_2 a_3 > a_3^2 + a_1^2 a_4$, to be satisfied,

we will assume the following:

$$a_3 < a_1 a_2, \quad (54)$$

$$a_4 a_1^2 < ((c_1 + c_2 + c_3)(c_1 c_2 + c_2 c_3 + c_1 c_3 - A a_1) + \beta \alpha (A - c_1) - c_1 c_2 c_3) a_3. \quad (55)$$

By the right hand side of (55) can be rewritten as follows:

$$((c_1 + c_2 + c_3)(c_1 c_2 + c_2 c_3 + c_1 c_3 - A a_1) + \beta \alpha (A - c_1) - c_1 c_2 c_3) a_3 = (a_1 a_2 - a_3) a_3 \quad (56)$$

$$= a_1 a_2 a_3 - a_3^2. \quad (57)$$

Substituting (57) into (55), we get the following:

$$a_1^2 a_4 < a_1 a_2 a_3 - a_3^2. \quad (58)$$

By (54), we see that the right hand side of (58) is positive, thus the inequality of (58) holds. Rearranging (58), we get:

$$a_1 a_2 a_3 > a_1^2 a_4 + a_3^2. \quad (59)$$

Hence, our endemic equilibrium satisfies the Routh-Hurwitz criterion; thus it is locally asymptotically stable.

C Alternate Stability Condition

From our characteristic polynomial for (11), we set λ to 0 to find a bifurcation. From the characteristic polynomial with $\lambda = 0$, we have:

$$H^* = \pm \frac{\sqrt{(\beta \alpha c_2 c_3 + \beta \alpha \gamma - \mu_H c_1 c_2 c_3) \Lambda c_1 c_2 c_3}}{-(\beta \alpha c_2 c_3 + \beta \alpha \gamma \rho \sigma - \mu_H c_1 c_2 c_3)} \quad (60)$$

$$= \pm \sqrt{\frac{\Lambda c_1 c_2 c_3}{(\beta \alpha c_2 c_3 + \beta \alpha \gamma - \mu_H c_1 c_2 c_3)}} \quad (61)$$

$$= \pm \sqrt{\frac{\Lambda}{(\frac{\beta \alpha}{c_1 c_2 c_3} (c_2 c_3 + \gamma \rho \sigma) - \mu_H)}} \quad (62)$$

Substitute H^* from (5) to get:

$$H^* = \sqrt{-(H^*)^2} \quad (63)$$

If we assume that (9) holds, then H^* is positive, but then the right hand side of (63) is imaginary, which contradicts H^* being positive. Thus, there is no $\lambda = 0$ bifurcation.

D MATLAB code for Markov chain

```
function results = hawk_markov(evf,tf,H0,S0,I0,R0,sigma,flag)
% results = hawk_markov(evf,tf,H0,S0,I0,R0,sigma,flag)
%
% Last revised 7/28/11, 1:11am
%
% Runs a Markov process on a hawk population that consumes
% infected dove meat.
%
% Inputs:
% evf ~ maximum number of events
% tf ~ maximum number of days
% H0 ~ initial adult hawks
% S0 ~ initial susceptible fledgelings
% I0 ~ initial infected fledgelings
% R0 ~ initial recovered fledgelings
% sigma ~ infection rate in food (use a negative value to
%       default to ~42%)
% flag ~ whether to create a plot
%
% Outputs:
% results ~ a vector containing the following totals from
%         the simulation:
%   total birth events
%   total infection events
%   total recovery events
%   total susceptible natural death events
%   total infected natural death events
%   total recovered natural death events
%   total infected disease death events
%   total susceptible aging events
%   total recovered aging events
%   total adult death events
%   total immigration events
%   mean annual growth

% Parameters
muH = 1 / (365*5); % adult natural death rate
muJ = 0.36 / (365*2); % juvenile natural death rate
d = 0.41 / 40; % disease death rate
lambda = 1; % adult hawk immigration rate
```

```

b = (3.44 / 365 / 2) * (2/3) * 0.835; % average hatchling
%       per hawk
% dove infection rate based on our research
if (sigma < 0)
    sigma = 0.38*0.14 + 0.47*0.5 + 0.15*0.9;
end
rho = 8.9 * (1/3) * (1/10) * 0.83;
gamma = 0.59 / 40; % recovery rate
alpha = 1 / (365*2); % aging rate
ifood = rho * sigma; % overall chance of getting infected
%       from food every day

% Event totals
btot = 0; % total birth events
itot = 0; % total infection events
rtot = 0; % total recovery events
sntot = 0; % total susceptible natural death events
intot = 0; % total infected natural death events
rntot = 0; % total recovered natural death events
idtot = 0; % total infected disease death events
satot = 0; % total susceptible aging events
ratot = 0; % total recovered aging events
hntot = 0; % total adult death events
imtot = 0; % total immigration events

% Rows represent, in order:
%       adult, susceptible, infected, recovered
pop = zeros(4, evf); % initial population matrix
% Setting up the initial conditions
pop(:,1) = [H0; S0; I0; R0];
times = zeros(1, evf); % Times of each event
counter = 2;

% Annual stats
years = floor(tf/365); % number of full years
yearid = 1; % index of the current year
annual_pop = zeros(1, years+1); % adult population
annual_growth = zeros(1, years+1); % adult population growth

% The main loop
%       While we still have events left to calculate...
while (counter-1 < evf && times(counter-1) < tf)

```

```

% Shorthand names for each variable this loop
H = pop(1,counter-1);
Sj = pop(2,counter-1);
Ij = pop(3,counter-1);
Rj = pop(4,counter-1);
if (pop(1,counter-1) <= 0) % If there are no adults...
    error(['Simulation aborted at event number ' ...
          num2str(counter-1) ' (no adult hawks).']);
end

% Event probabilities
% total event rate
totrate = b*H + ifood*Sj + gamma*Ij + muj*(Sj+Ij+Rj) ...
          + d*Ij + alpha*(Sj+Rj) + muH*H + lambda/H;
brate = b*H / totrate; % rate of birth event
irate = ifood*Sj / totrate; % rate of infection event
rrate = gamma*Ij / totrate; % rate of recovery event
snrate = muj*Sj / totrate; % rate of susceptible
% natural death event
inrate = muj*Ij / totrate; % rate of infected natural
% death event
rnrate = muj*Rj / totrate; % rate of recovered natural
% death event
idrate = d*Ij / totrate; % rate of infected disease
% death event
sarate = alpha*Sj / totrate; % rate of susceptible
% aging event
rarate = alpha*Rj / totrate; % rate of recovered aging
% event
hnrate = muH*H / totrate; % rate of adult death event
immrate = lambda/H / totrate; % rate of immigration
% event

% Figuring out which event happens
event = rand;
schange = 0;
ichange = 0;
rchange = 0;
hchange = 0;
if (event < brate)
    schange = 1;

```

```

        btot = btot + 1;
elseif (event < brate+irate)
    schange = -1;
    ichange = 1;
    itot = itot + 1;
elseif (event < brate+irate+rrate)
    ichange = -1;
    rchange = 1;
    rtot = rtot + 1;
elseif (event < brate+irate+rrate+snrate)
    schange = -1;
    sntot = sntot + 1;
elseif (event < brate+irate+rrate+snrate+inrate)
    ichange = -1;
    intot = intot + 1;
elseif (event < brate+irate+rrate+snrate+inrate+ ...
        rnrate)
    rchange = -1;
    rntot = rntot + 1;
elseif (event < brate+irate+rrate+snrate+inrate+ ...
        rnrate+idrate)
    ichange = -1;
    idtot = idtot + 1;
elseif (event < brate+irate+rrate+snrate+inrate+ ...
        rnrate+idrate+sarate)
    schange = -1;
    hchange = 1;
    satot = satot + 1;
elseif (event < brate+irate+rrate+snrate+inrate+ ...
        rnrate+idrate+sarate+rarate)
    rchange = -1;
    hchange = 1;
    ratot = ratot + 1;
elseif (event < brate+irate+rrate+snrate+inrate+ ...
        rnrate+idrate+sarate+rarate+hnrate)
    hchange = -1;
    hntot = hntot + 1;
else
    hchange = 1;
    imtot = imtot + 1;
end
% Evaluating the changes caused by the event

```



```

pop(:,counter) = [pop(1,counter-1)+hchange; ...
                 pop(2,counter-1)+schange;pop(3,counter-1)+ichange; ...
                 pop(4,counter-1)+rchange];

% Figuring out when the event happens
timeadd = exprnd(1/totrate);
times(counter) = times(counter-1) + timeadd;

% Annual stats
% If we've entered a new year...
if (times(counter-1) >= (yearid-1)*365)
    % If we haven't recorded the adult population yet...
    if (annual_pop(yearid) == 0)
        annual_pop(yearid) = pop(1,counter-1);
        yearid = yearid + 1;
    end
end

counter = counter + 1;
end

if (years) % If we have at least a year of simulation...
    for i = 1:years % For each year...
        annual_growth(i+1) = annual_pop(i+1) / ...
            annual_pop(i);
    end
    avg_annual_growth = mean(annual_growth(2:end));
else
    avg_annual_growth = 0;
end

% Drop all the unfilled columns
times = times(1:counter-1);
pop = pop(:,1:counter-1);

results = [btot, itot, rtot, sntot, intot, rntot, ...
          idtot, satot, ratot, hntot, imtot, avg_annual_growth];

% Plotting the results
if (flag)
    figure;
    hold on;

```

```
stairs(times,pop(1,:), 'r');  
stairs(times,pop(2,:), 'b');  
stairs(times,pop(3,:), 'k');  
stairs(times,pop(4,:), 'g');  
legend('H', 'S', 'I', 'R', 2);  
xlabel('time (days)');  
ylabel('hawk population');
```

```
end
```